

# Exploring effective interactions through transition charge density study of $^{70,72,74,76}\text{Ge}$ nuclei.

A. Shukla, P. K. Raina, P. K. Rath <sup>a</sup>

Department of Physics and Meteorology, IIT Kharagpur-721302, India.

<sup>a</sup>Department of Physics, University of Lucknow, Lucknow-226007, India.

December 22, 2018

## Abstract

Transition charge density (TCD) for  $0^+ \rightarrow 2_1^+$  excitation have been calculated for  $^{70,72,74,76}\text{Ge}$  nuclei within microscopic variational framework employing  $2p_{3/2}$ ,  $1f_{5/2}$ ,  $2p_{1/2}$  and  $1g_{9/2}$  valence space. The calculated TCDs for different monopole variants of Kuo interaction are compared with available experimental results. Other systematics like reduced transition probabilities  $B(E2)$  and static quadrupole moments  $Q(2)$  are also presented. It is observed that the transition density study acts as a sensitive probe for discriminating the response of different parts of effective interactions.

Keywords : Hartree Fock Bogoliubov, Effective Interactions, Transition charge density

Pacs Nos: 21.60.-n, 21.10.-k, 23.20.-g, 27.50.+e

## 1 INTRODUCTION

Inelastic electron scattering experiments restricted by low beam energies, provided much useful information on spins of particles, moment of the nuclear transitions such as electromagnetic transition probabilities and transition radii. Most of the electron scattering results were interpreted in terms of macroscopic models with a common feature of transition densities having surface peak. There is no a priori reason for the transition density to have a surface peaked shape, rather, the existence of interior peak may be a stringent test for any microscopic calculation. The advent of high-resolution techniques has made it possible to observe the transition densities for different excitations in the interior of nucleus [1]. It has opened up a new and powerful way to check the nuclear structure calculations with high precision. Recently, Richter [2] and Neumann-Cosel [3] have provided a state-of-the-art of inelastic electron scattering experiments and its potential to explore the subtle nuclear structure effects having close relations to the key problems of nuclear physics. Very recently Radhi [4] has also shown that this technique helps much in discriminating the finer effects of two body interactions and core-polarisation even in s-d shell nuclei when shape transitions become important.

Shell model has a potential to explore the physical phenomenon behind some unexpected experimental observations in different nuclear properties. One can have microscopic understanding of the dynamics through comparison of experimental results with the model calculations having specific varied ingredients. An example where such a study has been carried through is that of TCD for even-even Ni nuclei. Yokoyama and Ogawa [5, 6] carried out a shell model study within in  $(2p_{3/2}, 1f_{5/2}, 2p_{1/2})^n$  configuration. Working with three different effective interactions and looking at the effect of p-h excitation from  $(1f_{7/2})$  they concluded that the effective charge model which gave satisfactory description of  $B(E2)$  and  $Q(2)$  values, completely failed in describing the TCD. One gets an interior peak that is some times even larger than surface peak. They could analyse the microscopic origin of peak by looking at the contribution of  $0\hbar\omega$  and  $2\hbar\omega$  separately. The phases of individual contributions to TCD in these cases for the interior

peak were found to be opposite than that for the surface peak. Thus the combined result leads to desired experimental behaviour of small peak inside and large peak at the surface. This phase dependence of the TCD contributions from different intrinsic phenomenon makes their study sensitive.

Two different approaches have been evolved in literature to handle nucleon-nucleon (N-N) effective interactions within many body interaction framework for microscopic studies of nuclear properties. One of them, initiated more than thirty years ago by Kuo and Brown [7] is based on the different N-N forces and the regularization methods. This technique has been developed and applied in computing the effective interactions in different shells and is still being pursued actively. On the other hand, the possibility of separation of nucleonic interaction Hamiltonian into multipole fields too has been of quite interest from earliest times [8, 9, 10, 11]. Some recent studies [12, 13] have attempted to identify the importance of lower multipoles and their strengths through P+QQ interactions and its extensions. They have been quite successful.

It has been noticed [14] that the nuclear Hamiltonian can be separated rigorously in to monopole and multipole fields. Monopole fields with few parameters describe saturation properties and spectroscopic properties very well. Apart from their success [15, 16, 17] in describing binding energies and other global properties like M1, E2 and GT sum rules, they are also being used [16] as benchmarks for new promising approximations of solving large scale shell model problems in Monte Carlo methods [17, 18]. Monopole modifications have also been applied in f-p-g shell for the studies of double beta decay matrix elements of  $^{76}\text{Ge}$  and  $^{82}\text{Se}$  nuclei in variational framework [19] and shell model [20] apart from electron capture rates in astrophysics.

Hasegawa, Kaneko, Tazaki and Zhang have shown [12, 13] recently that P+QQ empirical effective interactions are very close to the realistic interactions provided J-independent proton-neutron (p-n) force is included properly. These studies have shown this equivalence explicitly in case of some p-f shell nuclei that is the best place [13] for such comparison. In case of medium mass (mass region 100) nuclei where shell model becomes unmanageable even with recent computation facilities there have not been much of the tested full shell effective interactions. So multipole field interactions have been the natural choice for microscopic variational models like Hartree-Fock, Hartree-Fock-Bogoliubov as well as bosonic models (different versions). There have been studies [22, 23], attempting to evolve some general trends of p-n interactions, which have led to the important conclusion that T=0 component of the interaction plays crucial role in describing microscopic properties. In particular, transition charge density studies [23] have acted as a sensitive way for fixing p-n component of Q.Q interaction.

Here we wish to demonstrate how this technique is very useful in discriminating between the role of different components of interactions. Inelastic electron scattering data in Germanium nuclei has shown some very interesting features [24] that have been explained in configuration mixing framework [25] of interacting boson model (IBM). There have been some microscopic attempts for the description of transition charge densities in various mass regions [1, 24, 26, 27, 28, 29, 5, 6]. Theoretical attempts in IBM, Shell model and Hartree-Fock-Bogoliubov (HFB) model have been made in literature to quite some extent with IBM acting as a convenient rather than microscopic framework. We present the theoretical study of transition charge densities for quadrupole excitation ( $0^+ \rightarrow 2_1^+$ ) in case of  $^{70,72,74,76}\text{Ge}$  nuclei in microscopic variational framework. Sensitivity of the first peak to specific variation of monopole strengths that result into the desired experimental observations, helps to identify the proper type and strengths of monopole changes on effective Kuo interactions in f-p-g valence space. This region which includes nuclei like Zn, Ge, Se, Kr, Sr and Zr show many interesting features from microscopic structure aspects in terms of shape transitions as well as deformations even in low lying states. These nuclei have been studied within variational models, restricted shell models and Bosonic models. We find that the study of transition charge densities is probably the finer way to explore effective interactions than other electromagnetic properties like spectra, BE(2) and Q(2) that have been extensively used in the literature.

## 2 CALCULATIONAL FRAMEWORK

The formalism to calculate the wavefunction  $|\Phi\rangle$  is based upon the Hartree-Fock-Bogoliubov (HFB) Method. The HFB theory generalizes and unifies the Hartree-Fock (HF) procedure (with HF field) and

the BCS Model (with pairing field) by treating them simultaneously on equal footing. The two-body hamiltonian  $H$  is given by

$$H = \sum_{\alpha} \epsilon_{\alpha} a_{\alpha}^{\dagger} a_{\alpha} + \frac{1}{4} \sum_{\alpha\beta\gamma\delta} \langle \alpha\beta | V | \gamma\delta \rangle a_{\alpha}^{\dagger} a_{\beta}^{\dagger} a_{\delta} a_{\gamma} \quad (1)$$

Axially symmetric HFB intrinsic state with  $K=0$  can be written as

$$|\Phi_0\rangle = \prod_{im} (U_{im} + V_{im} b_{im}^{\dagger} b_{i\bar{m}}^{\dagger}) |0\rangle \quad (2)$$

where the creation operators  $b_{im}^{\dagger}$  and  $b_{i\bar{m}}^{\dagger}$  are given by

$$b_{im}^{\dagger} = \sum_{\alpha} c_{i\alpha, m} a_{\alpha}^{\dagger} \quad \text{and} \quad b_{i\bar{m}}^{\dagger} = \sum_{\alpha} (-1)^{j-m} c_{i\alpha, m} a_{\alpha, -m}^{\dagger} \quad (3)$$

Using the standard projection technique, a state with good angular momentum is obtained from the HFB intrinsic state through the relation.

$$\begin{aligned} |\Psi_{MK}^J\rangle &= P_{MK}^J |\Phi_K\rangle \\ &= \left[ \frac{(2J+1)}{8\pi^2} \right] \int D_{MK}^J(\Omega) R(\Omega) |\Phi_K\rangle d\Omega \end{aligned} \quad (4)$$

where  $R(\Omega)$  and  $D_{MK}^J(\Omega)$  are the rotation operator and the rotation matrix respectively.

## 2.1 Static electromagnetic properties

Expressions used to calculate reduced transition probabilities  $B(E2)$  and static quadrupole moments  $Q(J^{\pi})$  are given below.

Employing the angular momentum projected wave-function  $|\Psi_K^J\rangle$ , one obtains the following expression for reduced transition probability  $B(E2)$

$$B(E2 : J_i \rightarrow J_f) = \left( \frac{5}{16\pi} \right) (e_{\pi} \langle Q_0^2 \rangle_{\pi} + e_{\nu} \langle Q_0^2 \rangle_{\nu})^2 \quad (5)$$

where

$$\begin{aligned} \langle Q_0^2 \rangle_{\tau_3} &= \langle \Psi_K^{J_i} | Q_0^2 | \Psi_K^{J_f} \rangle \\ &= [n^{J_i} n^{J_f}]^{-1/2} \int_0^{\pi} \sum_{\mu} \begin{pmatrix} J_i & 2 & J_f \\ -\mu & \mu & 0 \end{pmatrix} d_{-\mu 0}^{J_i}(\theta) n(\theta) \\ &\quad \times \left[ b^2 \sum_{\tau_3 \alpha \beta} e_{\tau_3} \langle \alpha | Q_{\mu}^2 | \beta \rangle \rho_{\alpha\beta}^{\tau_3}(\theta) \right] \sin\theta d\theta \end{aligned} \quad (6)$$

$$n(\theta) = \sqrt{\det[1 + M(\theta)]} \quad (7)$$

$$M(\theta) = F_{\alpha\beta}(\theta) f_{\alpha\beta}^{\dagger} \quad (8)$$

$$F_{\alpha\beta}(\theta) = \sum_{m'_{\alpha} m'_{\beta}} d_{m'_{\alpha}, m'_{\alpha}}^{j_{\alpha}}(\theta) d_{m'_{\beta}, m'_{\beta}}^{j_{\beta}}(\theta) f_{j_{\alpha} m'_{\alpha}; j_{\beta} m'_{\beta}} \quad (9)$$

$$f_{\alpha\beta} = \sum_i c_{ij_\alpha, m_\alpha} c_{ij_\beta, m_\beta} (V_{im_\alpha}/U_{im_\alpha}) \delta_{m_\alpha, -m_\beta} \quad (10)$$

$$n^J = \int_0^\pi n(\theta) d_{00}^J(\theta) \sin\theta d\theta \quad (11)$$

$$\rho_{\alpha\beta}^{\tau_3}(\theta) = [M(\theta)/(1 + M(\theta))]_{\alpha\beta}^{\tau_3} \quad (12)$$

and

$$Q_\mu^2 = \sqrt{\frac{16\pi}{5}} \frac{r^2}{b^2} Y_\mu^2(\theta, \phi) \quad (13)$$

Similarly the static quadrupole moments  $Q(J^\pi)$  are evaluated using the expression.

$$\begin{aligned} Q(J^\pi) &= \langle \Psi_K^J | Q_0^2 | \Psi_K^J \rangle \\ &= [n^J]^{-1} \begin{pmatrix} J & 2 & J \\ J & 0 & J \end{pmatrix} \int_0^\pi \sum_\mu \begin{pmatrix} J & 2 & J \\ -\mu & \mu & 0 \end{pmatrix} \\ &\quad \times d_{-\mu 0}^J(\theta) n(\theta) \left[ b^2 \sum_{\tau_3 \alpha \beta} e_{\tau_3} \langle \alpha | Q_\mu^2 | \beta \rangle \rho_{\alpha\beta}^{\tau_3}(\theta) \right] \sin\theta d\theta \end{aligned} \quad (14)$$

## 2.2 Transition Charge Density

The TCD,  $\rho_L(r)$  is the reduced matrix element of  $\rho_L^{op}$  between the initial and the final nuclear state of spin  $J_i$  and  $J_f$  and is given by

$$\rho_L(r) = \langle \Psi_K^{J_f} | \rho_L^{op} | \Psi_K^{J_i} \rangle \quad (15)$$

Employing the HFB wave functions, one obtains the following expression for TCD

$$\begin{aligned} \langle \Psi_K^{J_f} | \rho_L^{op} | \Psi_K^{J_i} \rangle &= [n^J n^{J'}]^{-\frac{1}{2}} \frac{(2J+1)}{2} \int_0^{\pi/2} \sum_\mu \begin{pmatrix} J & 2 & J' \\ -\mu & \mu & 0 \end{pmatrix} d_{-\mu 0}^J(\theta) \\ &\quad \times n(\theta) \left[ b^2 \sum_{\tau_3 \alpha, \beta} e_{\tau_3} R_{n_\alpha l_\alpha}(r) R_{n_\beta l_\beta}(r) \langle \alpha | Y_M^L | \beta \rangle(\theta) \right] \rho_{\alpha\beta}^{\tau_3} \sin\theta d\theta \end{aligned} \quad (16)$$

with

$$\rho_{\alpha\beta}^{\tau_3} = \left( M(\theta) [1 + M(\theta)]^{-1} \right)_{\alpha\beta}^{\tau_3} \quad (17)$$

and

$$n^J = \int_0^\pi \left[ \det \left( 1 + F^{(\pi)} f^{(\pi)\dagger} \right) \right]^{1/2} \left[ \det \left( 1 + F^{(\nu)} f^{(\nu)\dagger} \right) \right]^{1/2} d_{00}^J(\theta) \sin(\theta) d\theta \quad (18)$$

$b$  is the oscillator length parameter,  $R_{n_\alpha l_\alpha}(r)$  are harmonic oscillator wave-functions and  $e_{\tau_3}$  is effective charge.

The calculations have been performed with Kuo effective interaction operating in the valence space spanned by  $2p_{3/2}$ ,  $1f_{5/2}$ ,  $2p_{1/2}$  and  $1g_{9/2}$  orbits. The doubly closed nucleus  $^{56}\text{Ni}$  is treated as an

inert core. The relevant effective two-body interaction that we have employed is a renormalized G-matrix due to Kuo [30]. The single particle energies taken (in MeV) are  $\epsilon(2p_{3/2}) = 0.00$ ,  $\epsilon(1f_{5/2}) = 0.78$ ,  $\epsilon(2p_{1/2}) = 1.08$  and  $\epsilon(1g_{9/2}) = 3.50$ .

These interactions have been used for satisfactory explanation of the observed anomalous high-spin sequence in  $^{60}\text{Ni}$  with shell model calculations as well as for the theoretical studies of electromagnetic properties of the yrast and yrare states in Zn, Ge, Se and Kr isotopes [31]. Quite extensive studies of static properties of Germanium and Selenium isotopes in the microscopic variational framework have been reported [32, 33]. We present the results of projected HFB calculations for the transition charge densities, transition probabilities BE(2) and static quadrupole moment Q(2) for even-even  $^{72-76}\text{Ge}$  nuclei in next section and discuss how transition charge density calculations can be used in identifying monopole strengths.

### 3 RESULTS AND DISCUSSION

Two-body interaction matrix elements used in the calculation of electromagnetic and weak interaction properties, as discussed in the introduction, form a very essential and most important input to any nuclear model calculations. Let us look at the evolution of these two body interactions in the f-p valence space. From the literature we can notice that the use of two body interactions has been of considerable interest to many theoretical attempts in f-p and f-p-g shell for the description of energy spectrum, multipole moments and the transition probabilities for more than three decades. The realistic interaction for the f-p shell nuclei was constructed by Kuo and Brown [7] and put to test successfully for extracting the spectra of some nuclei near shell closure. Then exhaustive spectroscopic shell model calculations for Ca nuclei by McGrory, Wildenthal and Halbert [34] revealed that these interactions have to be modified slightly suggesting that the effective interaction for  $f_{7/2}$  with other orbits of the space are too strong. The next attempt made in modifying these effective interactions in f-p region was made by Sharma and Bhatt [35] to examine the intrinsic structure of even-even nuclei of Ti, Cr, and Fe. Based on these results and Nilsson structure of the orbits they suggested, in line with the MWH, that matrix elements for particles in  $(f_{7/2})^2$  should be made more attractive and the interaction of  $f_{7/2}$  with other orbits should be made more repulsive. The variation of these interaction matrix elements has been tried by them for 100, 200 and 300 KeV. Next very effective step in this development was that of monopole modifications [15]. The tremendous success of this modification in description of global properties and now using them for benchmarking of promising new techniques (like Monte Carlo) has established it as KB3 interaction. With the success of monopole modifications in f-p region, there have been now universal acceptability for them. Similar monopole modifications have been recently applied to the studies of double beta decay matrix elements of  $^{76}\text{Ge}$  and  $^{82}\text{Se}$  nuclei in variational framework [19] and shell model [20] employing f-p-g valence space. These are still considered to be one of the best microscopic nuclear matrix elements calculations in literature with the shell model nuclear matrix elements for neutrinoless double beta decay being taken as most reliable ones till date.

Ge nuclei have long presented challenge for microscopic description because of anomalous behaviour in energy systematics as well as transition charge densities of ground/low-lying states. There have been some discontinuous changes between neutron number N=40 to 42. IBM plus configuration mixing [25] has been applied successfully to the studies of systematics as well as transition charge densities. In these studies the idea of two different configuration has been evolved because of crucial role played by  $p_{3/2}$  and the  $f_{5/2}$  orbits. The calculations with restricted shell model [36, 37, 38], Variational models [31, 32] and IBM [24, 25] carried out in f-p-g region have shown that  $f_{5/2}$  orbits are playing very crucial role in describing static and dynamic properties. Truncated shell model calculations for N=50 (Zn-Rb) isotones in f-p-g valence space too indicate [36] that the occupancies of orbits are mainly dominated by  $f_{5/2}$  orbit followed by  $p_{3/2}$ . For lower mass region covering Zn to Zr nuclei it is found that the mixing with  $1f_{5/2}$  and  $2p_{3/2}$  orbits is very strong [37] and truncations excluding these levels may be justified only from mass 86 onwards. Very recently Langanke, Kolbe and Dean proposed [21] a new model to calculate stellar electron capture rates using the Shell Model Monte Carlo approach for even mass germanium isotopes in f-p-g valence space with pairing+quadrupole interaction. They adopted the single-particle energies from

the KB3 interaction but had to artificially reduce the  $f_{5/2}$  orbit by 1 MeV to simulate the effects of the  $\sigma\tau$  component that was missing in the residual interaction. This too points towards the need for larger occupancy of  $f_{5/2}$  orbit.

Taking a clue about the role of important orbits from these studies and looking at the success of monopole modifications in f-p region, we have attempted (restricting to yrast state excitations) transition charge densities for all Ge nuclei that have been studied experimentally. Though yrare excitations too are very interesting but are believed to be connected to the shape transitions and here we have confined ourselves with the studies of monopole effects. Specifically, to the identification of important orbits and finding their appropriate strengths. We explore the effect of monopole modification of effective two-body interaction with variation of strength by 100, 150, 200 and 250 keV. Kuo [30] interaction is denoted by Kuo00 effective interaction. Kuo00 has been modified by making  $\langle(f_{5/2})^2JT|V|(f_{5/2})^2JT\rangle$  interaction matrix elements attractive by 100 keV and  $\langle(p_{3/2})^2JT|V|(p_{3/2})^2JT\rangle$  interaction matrix elements repulsive by same amount (this modification is called Kuo10). Replacing 100 by 150, 200 and 250, we get Kuo15, Kuo20 and Kuo25 respectively. Detailed studies of transition charge density for first quadrupole excitation along with the static electromagnetic properties with respect to the variation of these monopole strengths in case of even-even  $^{70-76}\text{Ge}$  nuclei are presented in following subsections. We have tried different monopole modifications with different orbits as well as same/different strength variations for all orbits of the space, including the effect of transitions from/to  $p_{1/2}$  as well as  $g_{9/2}$  orbits. It is found that the combination that has been chosen is the best one to reproduce the desired characteristic of both peaks of TCDs simultaneously.

### 3.1 Static Electromagnetic Properties

#### 1. Total energy, Intrinsic Quadrupole Moment and Occupation Numbers

Table I presents the total HFB energy and total quadrupole moments (along with separate contribution from protons and neutrons) for  $^{70,72,74,76}\text{Ge}$  nuclei. Also presented are their variations with changes in monopole strengths discussed above.  $^{70,72}\text{Ge}$  nuclei show first increase in quadrupole moment and then decrease as we go from Kuo00 to Kuo25. Whereas,  $^{74,76}\text{Ge}$  nuclei show decreasing trend except for  $^{74}\text{Ge}$  at Kuo00 to Kuo10 where it hardly shows any change. Table II shows the change in proton and neutron occupation numbers in  $2p_{3/2}$ ,  $1f_{5/2}$ ,  $2p_{1/2}$  and  $1g_{9/2}$  orbits as we go on increasing monopole strength from 000 to 250 in steps. As expected we find promotion of particles from  $p_{3/2}$  to  $f_{5/2}$  orbits both for protons and neutrons. We notice that the occupancy of protons is almost completely governed by  $1f_{5/2}$  orbit with little bit spreading into  $2p_{3/2}$  and  $1p_{1/2}$  in case of Kuo25. Whereas, at Kuo20 some of them shift to  $2p_{3/2}$  and also occupy little bit of  $1g_{9/2}$  (seen in case of  $^{70,72}\text{Ge}$ ). Additional neutrons mainly keep occupying  $1g_{9/2}$  in going from  $^{70}\text{Ge}$  to  $^{76}\text{Ge}$ . There is not much change in neutron occupancies of  $2p_{1/2}$  and  $1g_{9/2}$  orbits while going from Kuo00 to Kuo25 and expected variation in other two orbits is similar to those of protons. The effects of these transitions of neutrons and protons into different orbits have been reflected on TCDs, B(E2) and Q(2) discussed in details in the following sections.

#### 2. Reduced Transition Probabilities B(E2) and Quadrupole Moments Q(2)

The calculated as well as experimentally observed values for the reduced transition probabilities B(E2;  $0^+ \rightarrow 2_1^+$ ) and static quadrupole moments Q(2 $^+$ ) for  $^{70,72}\text{Ge}$  are presented in Table I. The calculated results with effective charges  $e_{eff} = e_\nu=0.1$  and 0.2 along with those for different variants of Kuo00 are given in two columns. A closer look at the values shows that the changes from Kuo00 to Kuo25 in case of  $^{70}\text{Ge}$  increases BE(2) values in going from Kuo00 to Kuo10 and then keeps decreasing. In case of  $^{72}\text{Ge}$  nucleus the values at Kuo00 and Kuo10 are nearly same and then go on decreasing monotonically. The set of  $^{74,76}\text{Ge}$  nuclei have quite different behaviour from that of  $^{70,72}\text{Ge}$  in two respects. First, the values keep on decreasing very fast in going from Kuo00 to Kuo25. Secondly, there is a need for change in effective charge by approximately 0.3 units to have the BE(2) values closer to those suggested by experiments. We find that the calculated values match well with experiments in case of Ku20/Kuo25 for all Ge nuclei (within the presented small variation of effective charges). Thus Kuo20/Kuo25 seems to

be an appropriate monopole modification. We notice that the  $B(E2)$  values change very fast with  $e_{eff}$  and thus one could also arrive at the agreement with experimental values without going for monopole modifications but changing effective charge for each nucleus. This is a normal practice followed where one treats  $e_{eff}$  as free parameter in calculation and fixes it by experimental data. We shall see in next section that this kind of parameterization does not help with TCD studies. Theoretically calculated values for  $Q(2)$  along with experimental results (with large error bars) are also tabulated in last three columns. Similar changes as seen for  $BE(2)$  are observed in this case too. Due to large error bars in experiments nothing conclusive can be said by comparison except that the qualitative trends are shown with the need for increment of  $e_{eff}$  by 0.3 in going from  $^{72}\text{Ge}$  to  $^{74}\text{Ge}$ .

### 3.2 Transition Charge Densities for $0^+ \rightarrow 2_1^+$ excitation

In figures 1(a) and 1(b) we have presented the results for  $0^+ \rightarrow 2_1^+$  transition charge densities of  $^{70,72,74,76}\text{Ge}$  nuclei. Experimental [24] and the calculated results with unmodified Kuo (Kuo00) as well as for four modified KB interactions discussed above are also shown on different curves of each figure. Experimental plots of transition charge densities (between solid lines with vertical bars standing for errors) for  $0^+ \rightarrow 2_1^+$  are characterized by one small peak in the interior around  $r = 1.25$  fm and a large surface peak at  $r = 4.25$  fm. The surface peak in case of  $^{70,72}\text{Ge}$  nuclei is smaller in comparison to  $^{74,76}\text{Ge}$  nuclei.

These experimental results have been attempted in IBM framework which has been quite successful in unified description of collective states. To describe transition densities in this framework one has to introduce boson densities and most of the experimental data goes as input e.g. in reference 24 four sets of experimental data out of total of eight available sets were used as inputs. Whereas, shell model and variational model calculations have direct link with effective interactions; the changes in occupancies of protons from a specific orbit to the different orbits are displayed through transition charge density in a very sensitive way.

Figures 1(a) and 1(b) show the variation of transition charge densities for  $0^+ \rightarrow 2_1^+$  excitation in case of  $^{70,72}\text{Ge}$  and  $^{74,76}\text{Ge}$  nuclei respectively. Here effective charges for  $^{70,72}\text{Ge}$  and  $^{74,76}\text{Ge}$  nuclei are taken to be  $(e_\pi, e_\nu) = (1.15, 0.15)$  and  $(1.45, 0.45)$  respectively so as to give the surface peak matching with experimental values. In case of iso-scalar ( $e_\pi - e_\nu = 1.0$ ) effective charge interpretation one associates the effect of non-zero effective charge  $e_{eff} = e_\nu$  physically with core polarization. Thus the required change of effective charge by 0.3 in going from  $^{72}\text{Ge}$  to  $^{74}\text{Ge}$  shows the need for more core polarization in going from  $N=40$  to 42 nuclei. This change is quite noticeable on experimental results. Since  $N=40$  is not a good core and the monopole modifications hardly affect surface peaks, it indicates some important role being played by p-n interactions at  $N=40$ .

Now let us concentrate on the first peak. Transition charge densities with Kuo00, Kuo10, Kuo15, Kuo20 and Kuo25 interaction are plotted with dotted, dashed, crosses on solid, circles on solid and triangles on solid curves respectively. Theoretical results show that the first peak is very large in case of Kuo00 interaction (i.e. without any modification). Very interesting feature of this peak is its sensitivity to small variations in monopole strengths of orbits  $1f_{5/2}$  and  $2p_{3/2}$ . As we go on increasing the monopole strength by 100keV and then in steps of 50 keV the peak goes on decreasing and approaches towards experimental behaviour very fast. This is a general trend shown in case of all nuclei till Kuo20 though there appears to be somewhat better correspondence with experimental results even beyond 200 in case of  $^{70,72}\text{Ge}$ . As we go to  $^{74}\text{Ge}$  we find the peak almost stagnated at Kuo20, thus suggesting Kuo20/Kuo25 to be the appropriate monopole strength modification. Minima of calculated values between two peaks is found to be deviating from experimental curve and other detailed overall differences are expected to be due to the finer effects of higher order contributions that have not been represented exactly in Kuo interactions. In earlier elaborate variational model calculations on Ge nuclei [39, 40] the computed  $BE(2)$  and  $Q(2)$  values needed the variation of effective charges from nucleus to nucleus for better agreement with experimental results. One important reason for it appears to be the non-inclusion of appropriate monopole strength.

Even-even  $^{64-68}\text{Zn}$  nuclei studied [29] earlier within full f-p shell employing MWH [34] interactions displayed similar behaviour as discussed above for Ge nuclei with Kuo interaction. There it was understood as a consequence of limiting valence space that excluded  $g_{9/2}$  orbit. Other possible explanation for

large interior peak was believed to be the contribution from higher multipole interactions. The purely empirical Tassie model [39, 40], where one adds core polarization transition charge density given by the derivative of ground state charge density, was seen to provide better fitting with the experiments. This purely empirical model does not shed any light on microscopic phenomenon responsible for suppression of interior peak like the one demonstrated [6] in case of TCD for Ni isotopes. Our study of TCD in case of  $^{64,66,68}\text{Zn}$  nuclei, in same framework as discussed above for Ge nuclei, shows that these monopole modifications have a similar role to play in these nuclei too, thus showing that the contribution to quadrupole TCD amplitude due to particles in  $1p_{3/2}$  has same phase for interior and the surface region while it is in opposite phase in case of  $1f_{5/2}$  orbit. Thus we can very clearly say that the desired experimental behaviour for the TCDs of Ge nuclei in particular and other neighbouring nuclei in general show dominant occupancy in  $1f_{5/2}$  orbit.

## 4 SUMMARY AND CONCLUSION

Microscopic variational model calculations of transition charge density for  $0^+ \rightarrow 2^+$  excitation, transition probabilities  $B(E2)$  and static quadrupole moment  $Q(2)$  have been reported for  $^{70,72,74,76}\text{Ge}$  nuclei. The valence space  $2p_{3/2}$ ,  $1f_{5/2}$ ,  $2p_{1/2}$  and  $1g_{9/2}$  along with Kuo interaction has been used. The successes of monopole modifications on KB interactions (KB3 interaction) in f-p shell has prompted us to look for some better way to extract the strengths for such modifications in f-p-g shell. Germanium nuclei have long presented challenge for microscopic description because of anomalous behaviour in energy systematics as well as transition charge densities. IBM with two different configurations has been successfully evolved to study these anomalies where the role of mixing between  $p_{3/2}$  and the  $f_{5/2}$  orbits is found to be crucial. Shell model studies in this region too have shown the importance of occupancies of  $f_{5/2}$  orbits. With these observations in mind, we have examined the changes in transition charge densities with variation of strength by 100, 150, 200 and 250 keV for  $\langle (f_{5/2})^2 JT | V | (f_{5/2})^2 JT \rangle$  and  $\langle (p_{3/2})^2 JT | V | (p_{3/2})^2 JT \rangle$  interaction matrix elements. It is seen explicitly that the transition densities of inner peak are very sensitive to these changes whereas the surface peak is almost inert. The desired variations in inner peak of transition density so as to have observed experimental behaviour of small inner peak and large surface peak in case of  $^{70,72,74,76}\text{Ge}$  nuclei suggest Kuo25/Kuo20 to be the appropriate monopole modification strength.

## References

- [1] J. Heisenberg, *Advances in Nuclear Physics*, Vol. 12 (Plenum New York, 1981) 61.
- [2] A. Richter, *Prog. Part. Nucl. Phys.* **44**, 3 (2000).
- [3] P. von Neumann-Cosel, *Nucl. Phys.* **A690**, 52c (2001); *Prog. Part. Nucl. Phys.* **44**, 49 (2000).
- [4] R.A. Radhi, *Nucl. Phys.* **A707**, 56 (2002); et al. **A696**, 442 (2001).
- [5] A. Yokoyama and K. Ogawa, *Phy. Rev.* **C39**, 2458 (1989).
- [6] A. Yokoyama and K. Ogawa, *Phy. Rev.* **C42**, 1399(1990).
- [7] T.T.S. Kuo and G.E. Brown, *Nucl. Phys.* **A114**, 241 (1968).
- [8] L.S. Kisslinger and R.A. Sorensen, *Rev. Mod. Phys.* **35**, 853 (1963).
- [9] M. Baranger and K. Kumar, *Nucl. Phys.* **A110**, 529 (1968); **A122**, 241 (1968); **A122**, 273 (1968).
- [10] T. Kishimoto and T. Tamura, *Nucl. Phys.* **A192**, 246 (1972); **A270**, 317 (1976).
- [11] A. Bohr and B. Mottelson, *Nuclear Structure*, Benjamin, Reading, MA, 1975, Vol. 2.



- [12] M. Hasegawa, K. Kaneko and S. Tazaki, arXiv:nucl-th/0008007. Nucl. Phys. **A688**, 765 (2001).
- [13] M. Hasegawa, K. Kaneko and S. Tazaki, Nucl. Phys. **A674**, 411 (2000).
- [14] A. Abzouzi, E.Caurier and A.P. Zuker, Phys. Rev. Lett. **66**, 1134 (1991).
- [15] A. Poves and A.P. Zuker, Phys. Rep. **70**, 235 (1981).
- [16] E. Caurier, G. Martinez-Pinedo, F. Nowacki, A. Poves, J. Retamosa, and A.P. Zuker Phys. Rev. **C59**, 2033 (1999).
- [17] S.E. Koonin, D.J. Dean, and K. Langanke, Phys. Rep. **278**, 1 (1997).
- [18] M. Honma, T. Mizusaki, and T. Otsuka, Phys. Rev. Lett. **77**, 3315 (1996).
- [19] S.K. Dhiman and P.K. Raina, Phy. Rev. **C50**, R2660 (1994).
- [20] E. Caurier, F. Nowacki, A. Poves, and J. Retamosa, Phys. Rev. Lett. **77**, 1954 (1996).
- [21] K. Langanke, E. Kolbe and D.J. Dean, arXiv nucl-th/0012036. Phy. Rev. **C63**, 032801 (2001).
- [22] D.S. Brenner, C. Wesselborg, R.F. Casten, D.D. Warner, and J.Y. Zhang, Phys. Lett. **B243**, 1 (1990).
- [23] A.J. Singh, P.K. Raina and S.K. Dhiman, Phy. Rev. **C50**, 2307 (1994); A.J. Singh and P.K. Raina, Phy. Rev. **C52**, R2342 (1995).
- [24] J. P. Bazantay et al., Phy. Rev. Lett. **54**, 643 (1985).
- [25] P.D. Duval, D. Goutte and M. Vergnes, Phys. Lett. **B124**, 297 (1983).
- [26] O. Schwenker et al., Phy. Rev. Lett. **50**, 15 (1983).
- [27] J. Wesseling et al., Phys. Lett. **B245**, 338 (1990); J. Wesseling et al., Nucl. Phys. **A535**, 285 (1991).
- [28] T.E. Milliman et al., Phy. Rev. **C41**, 2586 (1990); J.P. Connelly et al., Phy. Rev. **C42**, 1948 (1990).
- [29] P.K. Raina and S.K. Sharma, Phy. Rev. **C37**, 1427 (1988).
- [30] T.T.S. Kuo, privatecommunication.
- [31] D.P. Ahalpara and K.H. Bhatt, Phys. Rev. **C25**, 2072 (1982).
- [32] P.N. Tripathi and S.K. Sharma, Phy. Rev. **C34**, 1081 (1986).
- [33] P.K. Rath and S.K. Sharma, Phy. Rev. **C38**, 2928 (1988).
- [34] J.B. McGrory, B.H. Wildenthal and E.C. Halbert, Phys. Rev. **C2**, 186 (1970).
- [35] Satish Sharma and Kumar Bhatt, Phys. Rev. Lett. **30**, 620 (1973).
- [36] Xiangdong Ji and B.H. Wildenthal, Phys. Rev. **C40**, 389 (1989).
- [37] C.J. Lister, P.J. Ennis, A.A. Chishti, B.J. Varley, W. Gelletly, H.G. Price and A.N. James, Phys. Rev. **C42**, R1191 (1990).
- [38] H. Hendel and B.A. Brown, Nucl. Phys. A **627**, 35 (1997).
- [39] L.J. Tassie, Aust. J. Phys. **9**, 407 (1956).
- [40] B.A. Brown, R. A. Radhi and B.H. Wildenthal, Phys. Rep. **101**, 313 (1983).

Table I. The calculated values of total energy (in MeV), intrinsic quadrupole moment (in units of  $b^2$ ),  $B(E2; 0^+ \rightarrow 2_1^+)$  (in units of  $e^2b^2$ ) and static quadrupole moment  $Q(2)$  (in units of  $b$ ) for the ground state HFB solution of  $^{70,72,74,76}\text{Ge}$  nuclei. Here  $\langle Q_0^2 \rangle_\pi$  and  $\langle Q_0^2 \rangle_\nu$  are separate contribution of the protons and neutrons respectively.

| Nucleus          | Interaction | $E_{HFB}$ | $\langle Q_0^2 \rangle_{HFB}$ | $\langle Q_0^2 \rangle_\pi$ | $\langle Q_0^2 \rangle_\nu$ | B(E2; $0 \rightarrow 2_1^+$ ) |       |                    |             | Q(2)  |                    |
|------------------|-------------|-----------|-------------------------------|-----------------------------|-----------------------------|-------------------------------|-------|--------------------|-------------|-------|--------------------|
|                  |             |           |                               |                             |                             | Theory                        |       | Expt. <sup>1</sup> | Theory      |       | Expt. <sup>2</sup> |
|                  |             |           |                               |                             |                             | $e_\pi=0.1$                   | 0.2   |                    | $e_\nu=0.1$ | 0.2   |                    |
| $^{70}\text{Ge}$ | Kuo25       | -27.29    | 28.49                         | 10.8                        | 17.7                        | 18.41                         | 22.76 | 17.90±0.30         | -0.17       | -0.19 | -0.09±0.06         |
|                  | Kuo20       | -26.47    | 29.69                         | 11.4                        | 18.3                        | 19.71                         | 24.46 | 17.70±4.60         | -0.18       | -0.20 |                    |
|                  | Kuo15       | -25.89    | 30.05                         | 11.9                        | 18.2                        | 20.88                         | 25.83 | 17.50±0.46         | -0.18       | -0.20 |                    |
|                  | Kuo10       | -25.53    | 29.62                         | 12.1                        | 17.6                        | 21.67                         | 27.02 |                    | -0.19       | -0.21 |                    |
|                  | Kuo00       | -25.49    | 26.34                         | 11.5                        | 14.8                        | 20.20                         | 25.40 |                    | -0.18       | -0.19 |                    |
| $^{72}\text{Ge}$ | Kuo25       | -29.39    | 27.79                         | 10.2                        | 17.6                        | 17.65                         | 21.80 | 20.80±0.30         | -0.17       | -0.18 | -0.13±0.06         |
|                  | Kuo20       | -28.26    | 28.98                         | 10.9                        | 18.1                        | 18.65                         | 23.15 | 22.27±0.49         | -0.17       | -0.19 |                    |
|                  | Kuo15       | -27.43    | 29.68                         | 11.5                        | 18.2                        | 20.08                         | 25.00 | 23.70±1.80         | -0.18       | -0.20 |                    |
|                  | Kuo10       | -26.89    | 29.79                         | 11.9                        | 17.9                        | 21.36                         | 26.64 |                    | -0.19       | -0.21 |                    |
|                  | Kuo00       | -26.51    | 28.39                         | 11.9                        | 16.5                        | 21.79                         | 27.43 |                    | -0.19       | -0.21 |                    |
| $^{74}\text{Ge}$ |             |           |                               |                             |                             | $e_\pi=0.4$                   | 0.5   |                    | $e_\nu=0.4$ | 0.5   |                    |
|                  | Kuo25       | -30.79    | 26.36                         | 9.7                         | 16.7                        | 29.53                         | 34.75 | 30.50±0.30         | -0.21       | -0.23 | -0.25±0.06         |
|                  | Kuo20       | -29.41    | 27.16                         | 10.2                        | 17.0                        | 31.90                         | 37.57 | 29.00±2.00         | -0.22       | -0.24 |                    |
|                  | Kuo15       | -28.27    | 27.92                         | 10.9                        | 17.0                        | 34.36                         | 40.57 | 30.00±3.20         | -0.23       | -0.25 |                    |
|                  | Kuo10       | -27.49    | 28.46                         | 11.6                        | 16.9                        | 37.54                         | 44.38 |                    | -0.24       | -0.26 |                    |
| Kuo00            | -26.77      | 28.21     | 12.0                          | 16.2                        | 41.23                       | 48.91                         |       | -0.25              | -0.28       |       |                    |
| $^{76}\text{Ge}$ | Kuo25       | -31.36    | 23.63                         | 9.2                         | 14.5                        | 27.63                         | 32.63 | 27.80±0.30         | -0.20       | -0.22 | -0.19±0.06         |
|                  | Kuo20       | -29.83    | 24.15                         | 9.6                         | 14.5                        | 29.71                         | 35.10 | 27.00±2.00         | -0.21       | -0.23 |                    |
|                  | Kuo15       | -28.45    | 24.77                         | 10.2                        | 14.6                        | 31.98                         | 37.82 | 26.00±0.50         | -0.22       | -0.24 |                    |
|                  | Kuo10       | -27.36    | 25.46                         | 11.0                        | 14.5                        | 34.89                         | 41.34 |                    | -0.23       | -0.25 |                    |
|                  | Kuo00       | -26.22    | 26.10                         | 11.8                        | 14.3                        | 40.22                         | 47.75 |                    | -0.25       | -0.27 |                    |

<sup>1</sup>S. Raman et al., Atom. Nucl. Data Tables **36** (1987) 41.

<sup>2</sup>P. Raghavan et al., Atom. Nucl. Data Tables **42** (1989) 189.

Table II. The calculated values of Occupation numbers of various sub-shell orbits for protons and neutrons for  $^{70,72,74,76}\text{Ge}$ .

| Nucleus          | Interaction | Protons    |            |            |            | Neutrons   |            |            |            |
|------------------|-------------|------------|------------|------------|------------|------------|------------|------------|------------|
|                  |             | $2p_{3/2}$ | $2p_{1/2}$ | $1f_{5/2}$ | $1g_{9/2}$ | $2p_{3/2}$ | $2p_{1/2}$ | $1f_{5/2}$ | $1g_{9/2}$ |
| $^{70}\text{Ge}$ | Kuo25       | 0.47       | 0.34       | 3.09       | 0.11       | 2.01       | 0.51       | 4.04       | 3.44       |
|                  | Kuo20       | 0.73       | 0.41       | 2.70       | 0.16       | 2.22       | 0.58       | 3.76       | 3.44       |
|                  | Kuo15       | 1.00       | 0.47       | 2.35       | 0.17       | 2.46       | 0.64       | 3.53       | 3.37       |
|                  | Kuo10       | 1.29       | 0.52       | 2.03       | 0.16       | 2.75       | 0.72       | 3.31       | 3.22       |
|                  | Kuo00       | 1.87       | 0.62       | 1.42       | 0.10       | 3.37       | 0.96       | 2.88       | 2.79       |
| $^{72}\text{Ge}$ | Kuo25       | 0.23       | 0.27       | 3.50       | 0.00       | 2.14       | 0.53       | 4.63       | 4.70       |
|                  | Kuo20       | 0.46       | 0.34       | 3.11       | 0.09       | 2.38       | 0.61       | 4.31       | 4.69       |
|                  | Kuo15       | 0.78       | 0.42       | 2.67       | 0.14       | 2.67       | 0.70       | 4.03       | 4.60       |
|                  | Kuo10       | 1.10       | 0.48       | 2.28       | 0.14       | 2.95       | 0.80       | 3.79       | 4.46       |
|                  | Kuo00       | 1.66       | 0.57       | 1.66       | 0.10       | 3.42       | 1.01       | 3.42       | 4.15       |
| $^{74}\text{Ge}$ | Kuo25       | 0.16       | 0.22       | 3.61       | 0.00       | 2.40       | 0.59       | 5.16       | 5.85       |
|                  | Kuo20       | 0.23       | 0.27       | 3.50       | 0.00       | 2.61       | 0.65       | 4.89       | 5.86       |
|                  | Kuo15       | 0.52       | 0.36       | 3.04       | 0.08       | 2.90       | 0.76       | 4.58       | 5.75       |
|                  | Kuo10       | 0.89       | 0.44       | 2.55       | 0.12       | 3.18       | 0.90       | 4.30       | 5.62       |
|                  | Kuo00       | 1.54       | 0.54       | 1.82       | 0.10       | 3.56       | 1.16       | 3.90       | 5.37       |
| $^{76}\text{Ge}$ | Kuo25       | 0.11       | 0.18       | 3.71       | 0.00       | 2.86       | 0.72       | 5.54       | 6.88       |
|                  | Kuo20       | 0.16       | 0.22       | 3.62       | 0.00       | 3.02       | 0.77       | 5.38       | 6.84       |
|                  | Kuo15       | 0.28       | 0.28       | 3.41       | 0.03       | 3.20       | 0.86       | 5.16       | 6.78       |
|                  | Kuo10       | 0.67       | 0.37       | 2.86       | 0.10       | 3.42       | 1.04       | 4.90       | 6.64       |
|                  | Kuo00       | 1.45       | 0.50       | 1.95       | 0.10       | 3.72       | 1.41       | 4.44       | 6.44       |

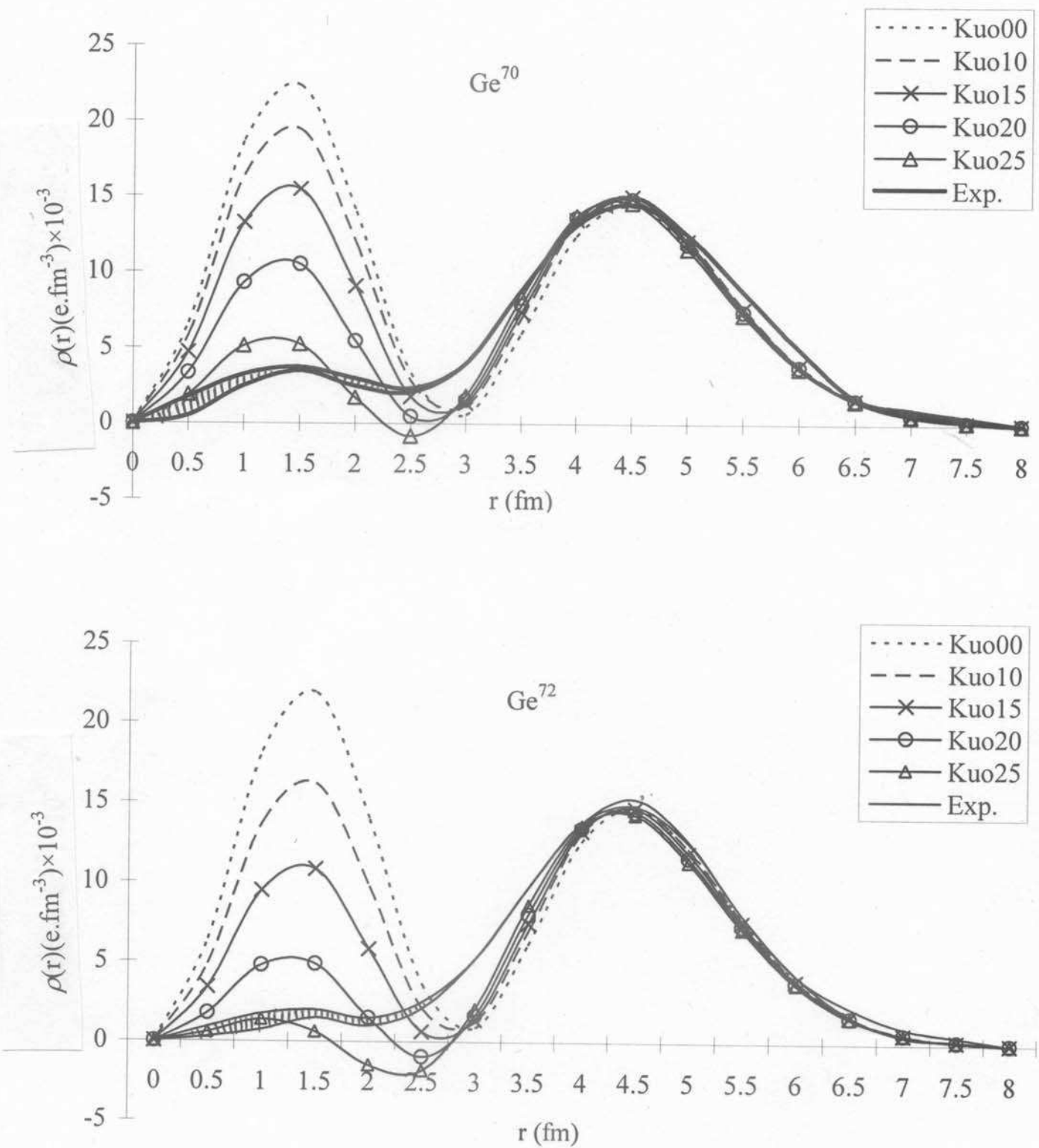


Figure 1(a). Variation of transition charge density ( $0^+ \rightarrow 2_1^+$  excitation) with monopole strengths modified by 100keV (Kuo10), 150keV (Kuo15), 200keV (Kuo20), and 250keV (Kuo25) on Kuo interaction (Kuo00) in case of  $^{70,72}Ge$  nuclei.

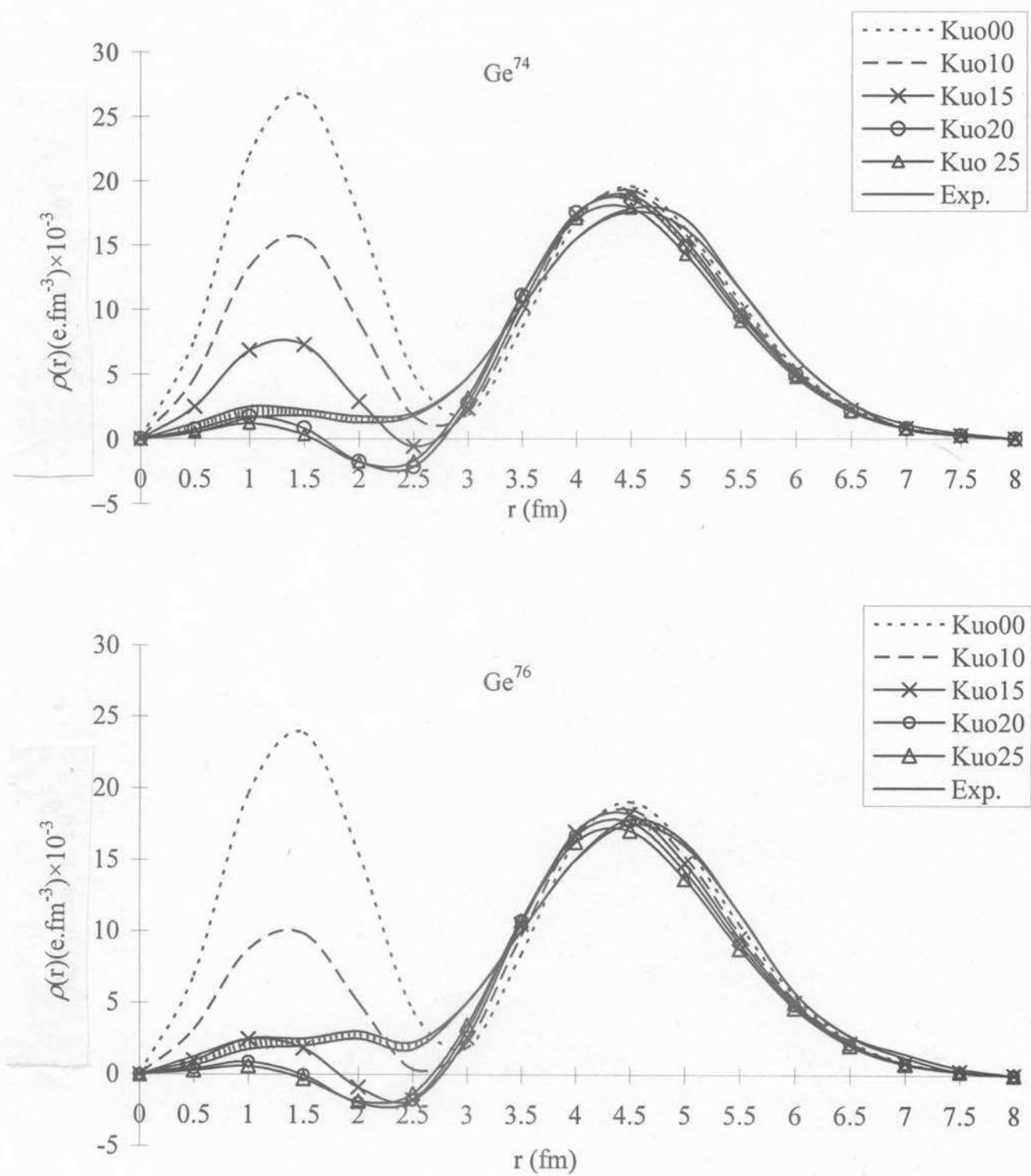


Figure 1(b). Variation of transition charge density ( $0^+ \rightarrow 2_1^+$  excitation) with monopole strengths modified by 100keV (Kuo10), 150keV (Kuo15), 200keV (Kuo20), and 250keV (Kuo25) on Kuo interaction (Kuo00) in case of  $^{74,76}Ge$  nuclei.